Magnetic, dielectric and magnetodielectric properties of PVDF-$La_{0.7}Sr_{0.3}MnO_3$ polymer nanocomposite film

Cite as: AIP Advances 3, 112109 (2013); https://doi.org/10.1063/1.4830282
Submitted: 12 August 2013 . Accepted: 31 October 2013 . Published Online: 07 November 2013

Ch. Thirmal, Chiranjib Nayek, P. Murugavel, and V. Subramanian

AIP ADVANCES **3**, 112109 (2013)

Magnetic, dielectric and magnetodielectric properties of PVDF-$La_{0.7}Sr_{0.3}MnO_3$ polymer nanocomposite film

Ch. Thirmal, Chiranjib Nayek, P. Murugavel,[a] and V. Subramanian
Department of Physics, Indian Institute of Technology Madras, Chennai 600036, India

(Received 12 August 2013; accepted 31 October 2013; published online 7 November 2013)

We have investigated the structure, magnetic and dielectric properties of PVDF-$La_{0.7}Sr_{0.3}MnO_3$ polymer nanocomposite thick film fabricated by dip coating technique along with the magnetodielectric effect. The structure and dielectric properties show the enhanced β phase in the composite compared to the PVDF film. The coupling between the ferroelectric and magnetic phases in the composite is revealed in the form of dielectric anomaly at the ferromagnetic Curie temperature. We observed 1.9% magnetodielectric effect at 300 K with the possibility of enhanced effect near the transition temperature. In addition, the analysis of the electric modulus indicates that the composite exhibits interfacial related relaxation and it follows Arrhenius Law. Our study suggests that the ac conductivity of the PVDF-$La_{0.7}Sr_{0.3}MnO_3$ composite could be explained by correlated barrier hopping mechanism. [http://dx.doi.org/10.1063/1.4830282]

I. INTRODUCTION

Interest in the field of magnetoelectrics gained momentum due to its fascinating physics and application potential in information storage, spintronics, multi-stage memories etc.[1] Though there are few single phase multiferroic materials exist in nature, their applications are limited either due to their order parameters existing at low temperatures[2] or due to difficulties in synthesizing them in stoichiometric form with low dielectric loss.[3] Alternatively, composites engineered from ferroelectric and magnetic phases show the product property with improved coupling between them.[4] Several ceramic composites made from the combination of ferroelectric $PbZr_xTi_{1-x}O_3$, $0.7PbMg_{1/3}Nb_{2/3}O_3$-$0.3PbTiO_3$, $BaTiO_3$ etc, and ferromagnetic $Tb_{1-x}Dy_xFe_2$, $NiFe_2O_4$, $CoFe_2O_4$, $La_{1-x}Sr_xMnO_3$ etc, show remarkable magnetoelectric properties.[5–12] However, the ceramic composites pose serious problems like inter-diffusion, chemical reaction and differential thermal expansion during high temperature processing (>1000 K) which limit their application potential. These problems can be overcome in polymer based composites where they are processed at temperatures below 500 K. Polyvinylidene fluoride (PVDF) is a known ferroelectric polymer and it crystallizes in α, β and γ polymorphs. Among them α-phase is non-polar, where β and γ phases are polar and show spontaneous polarization.[13] Composites like PVDF-Terfenol-D, PVDF-$CoFe_2O_4$, PVDF/La_2CoMnO_6, PVDF/ $Pr_{0.6}Ca_{0.4}MnO_3$ etc showed to exhibit reasonable magnetoelectric coupling.[14–17] Generally the composites are known to show enhanced magnetoelectric effect near the order parameter. To enhance the magnetoelectric effect and to maximize it near room temperature, it would be better to choose a ferromagnetic material with T_C higher than the room temperature but below the melting point of PVDF. In the reported PVDF based composites, the ferromagnetic order parameter is either well above the melting point of PVDF (433 K) (example: Terfenol-D and $CoFe_2O_4$) or well below room temperature (example: La_2CoMnO_6 and $Pr_{0.6}Ca_{0.4}MnO_3$), which constrain the possibility of tuning the magnetoelectric effect near room temperature. In this context, the $La_{1-x}Sr_xMnO_3$ compounds can be used to prepare a good magnetoelectric polymer composite since its Curie temperature

[a]Email: muruga@iitm.ac.in

(T_C) can be tuned from low temperature to 380 K by varying Sr content. As a first step, in the present work we have chosen $La_{0.7}Sr_{0.3}MnO_3$ whose T_C is 354 K as the magnetic phase and fabricated the magnetodielectric nanocomposite film by dispersing it in the PVDF matrix. The magnetodielectric coupling, dielectric and magnetic measurements are performed and the results are discussed in this paper.

II. EXPERIMENTAL

The $La_{0.7}Sr_{0.3}MnO_3$ (LSMO) in nanocrystalline form is synthesized by sol-gel route from the precursors such as lanthanum acetate, strontium carbonate and manganese acetate tetrahydrate. Stoichiometric amount of the precursors dissolved in nitric acid are mixed and stirred for 1 hrs at 60 °C. Appropriate amount of citric acid as gelating agent is added and stirred continuously for 3 hrs. Then 10 ml of ethylene glycol is added as polymerization agent and the mixture is stirred continuously till the brown color gel forms. This gel is taken into the crucible and heated at 400 °C for 2 hrs and then ground to get the powder form. The powder is calcined at 770 °C for 4 hrs to get LSMO powder. The PVDF powder (0.432 g: Average molecular weight 534000) is added to the solution containing 3 ml of acetone and 3 ml of N,N-dimethyle formamide and sonicated for 1 hr until colorless PVDF gel is formed. To fabricate the composite film with 30 weight percentage LSMO and 70 weight percentage PVDF, appropriate amount of LSMO is added to the PVDF gel and the gel is subjected to sonication for 3 hrs to homogenize the mixture. Since PVDF has good adhesion to aluminum, aluminum sheets cleaned by a series of sonication with the distilled water, ethanol and acetone for few minutes are used as substrates. After cleaning, the aluminum sheet is dipped in the gel for 1 minute and subjected heat treatment at 150 °C for 2 hrs to get the film. For comparison, we have also made pure PVDF film on aluminum sheet.

The fabricated films are subjected to various characterization tools. The morphology and thickness of the films are inferred from Quanta 400 FEG Scanning Electron Microscope and the phase formation is studied by employing Pananalytical X'Pert Pro X-ray diffractometer. Infrared spectrum is recorded using Bruker Alpha (ATR-IR) spectrometer and the magnetic measurements are carried out using Lakeshore Vibrating Sample Magnetometer. Silver conducting paint is used as top electrode on the film to make parallel plate configuration for studying the electrical properties. The fabricated films are subjected to dielectric constant, ac conductivity and electric modulus measurements using NumetriQ (PSM1375) phase sensitive multimeter.

III. RESULTS AND DISCUSSION

The morphology of the PVDF and PVDF-LSMO composite is shown in Fig. 1(a) and 1(b), respectively. Spherulitic structure of α-phase is seen on the surface of pure PVDF film.[18] However, is not prominently seen in the composite and rather uniform distribution of bright spots corresponding to the metallic LSMO particles dispersed in the PVDF matrix are seen. The images also confirm voids and porous free structure which is essential for electrical measurements. The thickness of the films as inferred from the cross-sectional image, shown as an inset in Fig. 1, is around 5 μm for both films.

The X-ray diffraction pattern (XRD) for the LSMO nanoparticles, PVDF and composite film on aluminum substrate are shown in Fig. 2. The diffraction peaks are indexed to PVDF and LSMO. The peaks at 18.1 and 20.1 represent (100) and (110) reflections of α-PVDF and the peak at 20.8 represents the (111) reflection of β-PVDF. The reduction in intensity of (110) reflection of the α-phase in the composite could be due to the decrease in the amount of α-phase.

To calculate the relative amount of β-phase in the composite film, we have taken Fourier transform infra red spectrum (FTIR) for pure PVDF and composite film and the results are shown in Fig. 3. The absorbencies at 614 cm^{-1}, 760 cm^{-1}, 795 cm^{-1}, 853 cm^{-1}, 974 cm^{-1}, 1071 cm^{-1}, and 1172 cm^{-1} correspond to α-PVDF and the absorbencies at 879 cm^{-1} and 838 cm^{-1} correspond to β-PVDF.[19–21] The relative amount of β-phase obtained from the formula $F(\beta) = A_\beta/(1.26A_\alpha + A_\beta)$ are 0.388 and 0.462 in pure PVDF and composite, respectively. A_β is the absorbance at 838 cm^{-1} and A_β is the absorbance at 760 cm^{-1}.[22] The increase in the amount of β-PVDF in the composite

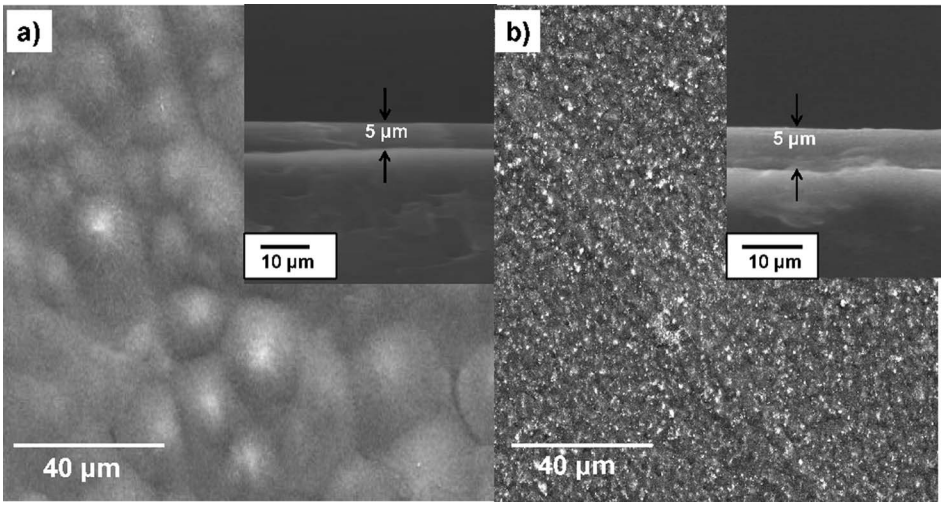

FIG. 1. SEM morphology of the (a) PVDF and (b) PVDF-$La_{0.7}Sr_{0.3}MnO_3$ composite. The inset shows the cross sectional image of the respective films.

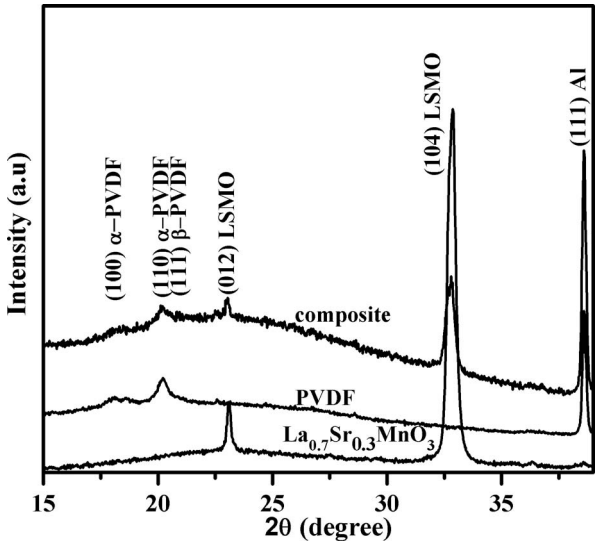

FIG. 2. XRD patterns of $La_{0.7}Sr_{0.3}MnO_3$ nanoparticles, PVDF and PVDF-$La_{0.7}Sr_{0.3}MnO_3$ composite.

could be due to the LSMO nanoparticles acting as additional nucleating site for the crystallization of β-phase.[23]

The PVDF-LSMO composite retains its magnetic properties of the parent LSMO nanoparticles. Room temperature magnetization versus the magnetic field curve shown in Fig. 4 indicates the ferromagnetic behavior of the film with 2.5 emu/cm^3 and 350 Oe as saturation magnetic moment and the coercive field, respectively. Note that the Curie temperature of the parent LSMO is at 354 K (the temperature variation of the magnetic moment of pure LSMO is shown as an inset in Fig. 4).

The dielectric constant and the loss tangent are measured for PVDF and PVDF-LSMO composite as a function of temperature from 300 K to 420 K at various frequencies are shown in Fig. 5. The increase in dielectric permittivity with increasing temperature indicates the existence of dipolar polarization in the samples.[24,25] Note that, the dielectric permittivity of the composite is higher than the pure PVDF. This can be attributed to the increment in the dipolar contribution because of increase in relative amount of β-phase (ferroelectric phase) in the composite as confirmed from the FTIR

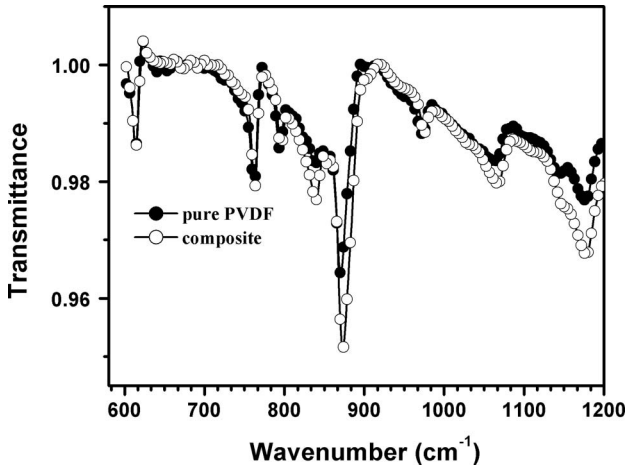

FIG. 3. FTIR spectrum of PVDF and PVDF-$La_{0.7}Sr_{0.3}MnO_3$ composite.

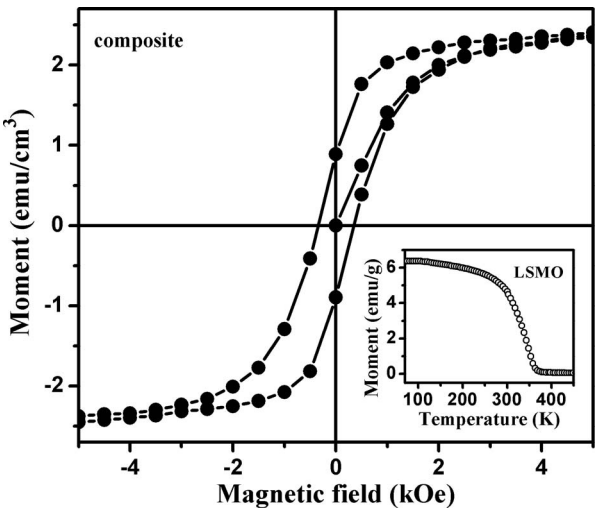

FIG. 4. Magnetization versus the magnetic field for the composite at 300 K and the inset shows the temperature variation of the magnetization for $La_{0.7}Sr_{0.3}MnO_3$ nanoparticles.

measurement. In addition, the interfacial polarization arising from the filler (LSMO nanoparticles) acting as trapping centers, may contribute to the enhancement in the dielectric constant of the composite.[26] Interestingly, the dielectric constant plot for the composite exhibit a clear anomaly at 354 K and it is independent of the frequency. The anomaly is also highly reflected in the loss tangent versus temperature graph at 354 K and it is frequency independent as shown in Fig. 5(b). The dielectric loss in the composite can be attributed to the metallic nature of the LSMO nanoparticles dispersed in the PVDF matrix.

To probe it further, we have plotted the dielectric constant, loss tangent and the derivative of magnetic moment as a function of temperature near the anomaly and the resultant graph is shown in Fig. 6. The anomaly at 354 K observed in the dielectric measurements is coinciding with the Curie temperature. The dielectric anomaly at magnetic ordering temperature can be attributed to the magnetodielectric coupling as reported in some of the single phase multiferroics[27] and in composites.[28] The large strain produced due to sudden change in the lattice parameter of ferromagnetic phase near its ordering temperature can be coupled to the ferroelectric phase through the elastic coupling.[28]

To quantify the magnetodielectric effect (MD), we have measured the dielectric constant of the composite as a function of the magnetic field in steps of 100 Oe at frequencies varies from 1 kHz to

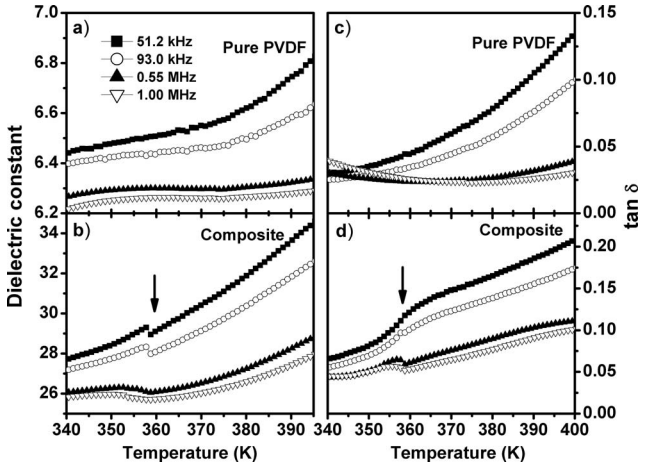

FIG. 5. The dielectric constant versus temperature plots for (a) PVDF and (b) composite. The dielectric loss versus temperature plots for (c) PVDF and (d) composite.

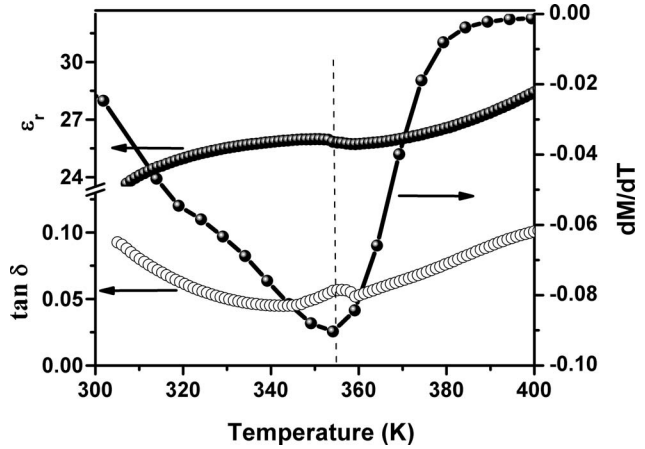

FIG. 6. The dielectric constant and dielectric loss as function of temperature for the composite and the dM/dT versus temperature for the $La_{0.7}Sr_{0.3}MnO_3$ nanoparticles.

500 kHz at 300 K. The magnetodielectric effect is calculated from $MD = \frac{\varepsilon_r(H)-\varepsilon_r(0)}{\varepsilon_r(0)} \times 100$, where $\varepsilon_r(0)$ and $\varepsilon_r(H)$ are the dielectric constants with and without magnetic fields (H), respectively. The resultant plot at various frequencies is shown in Fig. 7. The plot indicate the maximum of 1.9 % MD at 3.8 kOe which is comparable in magnitude with the reported values at the same field for similar such composites but at low temperatures.[16,17] It is known that maximum magnetodielectric coupling could be obtained near the transition temperature where the magnetostriction is high which enhances the strain mediated coupling.[16,28] Since the T_C of LSMO is at 354 K, we could expect high MD in the LSMO-PVDF composite near T_C. Our experimental limitations restrict the measurement only at room temperature. Alternatively, by selecting an appropriate LSMO composition, whose Curie temperature is near room temperature, it is possible to enhance in magnetodielectric effect near room temperature.

In order to understand the relaxation mechanism in this composite, the imaginary part of the electric modulus (M′) as a function of frequency at temperatures from 383 K to 423 K is shown in Fig. 8. The M″ indicates a relaxation behavior in this temperature range which could be correlated to the interfacial relaxation (Maxwell-Wagner- Scillars) mechanism in the polymer nanocomposite.[29] This relaxation follows the Arrhenius type,[30,31] $f = f_o \exp(-\Delta E/RT)$ where f_o is the constant, R is the gas constant and ΔE is the activation energy. The plot of $\log f$ versus $1000/T$ is shown on the left

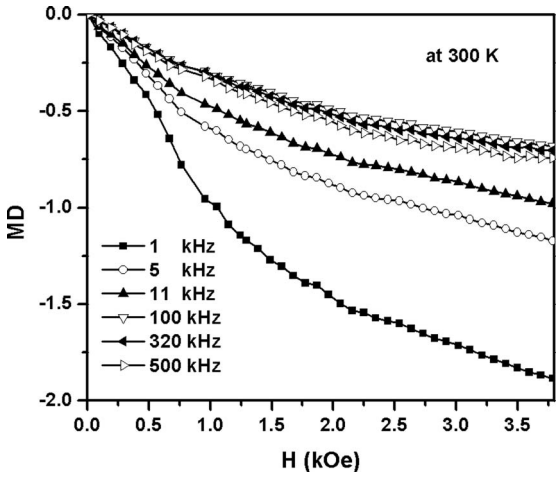

FIG. 7. The percentage change in dielectric constant (MD) as a function of magnetic field at 300 K is plotted at various frequencies.

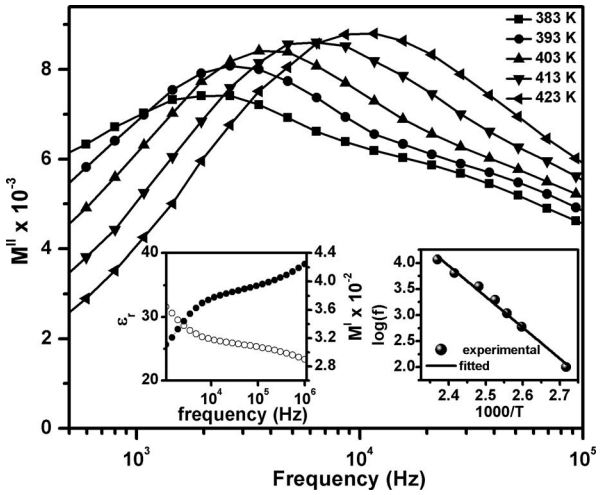

FIG. 8. M″ versus frequency plot for the composite at various temperatures and the left side inset shows the dielectric constant and M′ as a function of frequency and the right side inset shows log(f) versus 1000/T for the composite.

side inset of Fig. 8. The activation energy found from the slope is 1.18 eV. To verify the contribution coming from the electrode polarization effect, the frequency variation of dielectric permittivity and real part of the dielectric modulus (M′) at 300 K is shown as inset on the right of Fig. 8. The observed variations in the dielectric permittivity opposite to that of the variations in M′ with frequency clearly ascertain that there is no electrode polarization contribution.[32]

To understand the conduction mechanism in the PVDF-LSMO polymer composite, the ac conductivity is measured as a function of frequency at different temperatures. The plot of $\ln(\sigma_{ac})$ versus $\ln(\omega)$ is shown in Fig. 9. The graph is fitted with $\sigma = A\omega^S$, where A is the pre-exponential factor and S is the universal exponent. The temperature dependent of S is used to describe the conduction mechanism. If S is increasing with the increasing temperature, then the conduction mechanism can be explained by small polaron tunneling model and if it is decreasing with the increasing temperature, then conduction mechanism can be explained by correlated barrier hopping model.[33,34] The observed value of S is 0.66, 0.65, 0.62, 0.55, and 0.48 at 383 K, 393 K, 403 K, 413 K, and 423 K, respectively showing a decreasing trend with increasing the temperature. Hence the ac conduction mechanism in the PVDF-LSMO polymer composite could be explained by correlated barrier hopping mechanism.

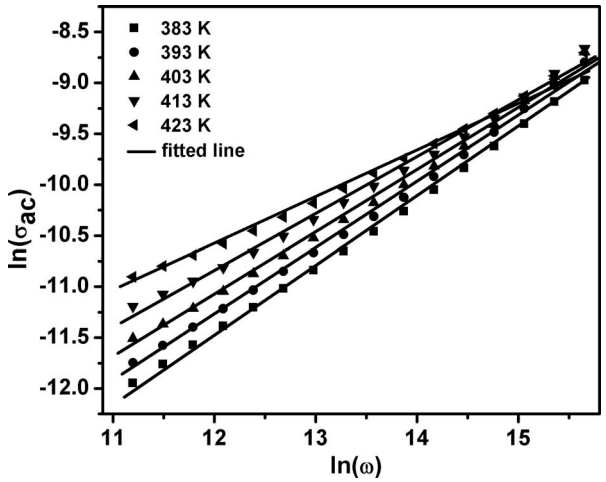

FIG. 9. Variation of ac conductivity (σ_{ac}) with frequency (ω) at different temperatures for the composite.

IV. CONCLUSION

The PVDF-$La_{0.7}Sr_{0.3}MnO_3$ polymer nanocomposite thick film fabricated by dip coating technique on aluminum substrate showed an enhanced crystallization of ferroelectric β-phase. This was also confirmed by an increase in the dielectric constant of the composite compared to the pure PVDF. The polymer nanocomposite exhibited an anomaly at 354 K, which coincided with the ferromagnetic to paramagnetic transition temperature of $La_{0.7}Sr_{0.3}MnO_3$, suggesting the possible coupling between the coexisting phases. The measured magnetodielectric effect show 1.9% change in dielectric constant under 3.8 kOe field at 300 K. We suggest that the enhanced magnetodielectric effect near room temperature could be obtained by tuning the $La_{1-x}Sr_xMnO_3$ composition. The electric modulus analysis carried out on the PVDF-$La_{0.7}Sr_{0.3}MnO_3$ polymer nanocomposite revealed that the relaxation mechanism shown by the composite could be attributed to the Maxwell - Wagner - Scillars interfacial relaxation. The ac conduction mechanism in the composite could be fit with the correlated barrier hopping mechanism.

[1] C. W. Nan, M. I. Bichurin, Shuxiang Dong, D. Viehland, and G. Srinivasan, J. Appl. Phys. **103**, 031101 (2008).
[2] L. W. Martin, S. P. Crane, Y. H. Chu, M. B. Holcomb, M. Gajek, M. Huijben, C. H. Yang, N. Balke, and R. Ramesh, J. Phys.: Condens. Matter. **20**, 434220 (2008).
[3] A. K. Pradhan, K. Zhang, D. Hunter, J. B. Dadson, G. B. Loiutts, P. Bhattacharya, R. Katiyar, J. Zhang, D. J. Sellmyer, U. N. Roy, Y. Cui, and A. Burger, J. Appl. Phys. **97**, 093903 (2005).
[4] G. Srinivasan, Annu. Rev. Matter. Res. **40**, 153 (2010).
[5] H. Ryu, P. Murugavel, J. H. Lee, S. C. Chae, T. W. Noh, Y. S. Oh, H. J. Kim, K. H. Kim, C. Bae, and J. G. Park, Appl. Phys. Lett. **89**, 102907 (2006).
[6] J. P. Zhou, H. He, Z. Shi, and C. W. Nan, Appl. Phys. Lett. **88**, 013111 (2006).
[7] C. W. Nan, N. Cai, L. Liu, J. Zhai, and Y. Lin, J. Appl. Phys. **94**, 5930 (2003).
[8] A. D. Sheikh and V. L. Mathe, J. Phys. Chem. Solids **72**, 1423 (2011).
[9] Y. Wang, S. W. Or, H. L. W. Chan, X. Zhao, and H. Luo, J. Appl. Phys. **103**, 124511 (2008).
[10] L. Hao, D. Zhou, Q. Fu, and Y. Hu, J. Mater. Sci. **48**, 178 (2013).
[11] Chiranjib Nayek, Kishor Kumar Sahoo, and P. Murugavel, Mater. Res. Bull. **48**, 1308 (2013).
[12] T. X. Li, M. Zhang, F. J. Yu, Z. Hu, K. S. Li, D. B. Yu, and H. Yan, J. Phys. D: Appl. Phys. **45**, 085002 (2012).
[13] E. Fukada and T. Furukawa, Ultrasonics January **31** (1981).
[14] K. Mori and M. Wutting, Appl. Phys. Lett. **81**, 100 (2002).
[15] P. Martins, C. M. Costa, G. Botelho, S. Lanceros-Mendez, J. M. Barandiaran, and J. Gutierrez, Mater. Chem. and Phys. **131**, 698 (2012).
[16] D. Bhadra, M. G. Masud, S. K. De, and B. K. Chaudhuri, Appl. Phys Lett. **102**, 072902 (2013).
[17] K. D. Chandrasekhar, A. K. Das, and A. Venimadhav, Appl. Phys. Lett. **98**, 122908 (2011).
[18] M. P. Silva, V. Sencadas, G. Botelho, A. V. Machado, A. G. Rolo, J. G. Rocha, and S. Lanceros-Mendez, Mater. Chem. and Phys. **122**, 87 (2010).
[19] Y. Bormashenko, R. Pogreb, O. Stanevsky, and E. Bormashenko, Polym. Test **23**, 791 (2004).
[20] A. K. Zak, W. C. Gan, W. H. A. Majid, M. Darroudi, and T. S. Velayutham, Ceram. Int. **37**, 1653 (2011).
[21] T. Boccaccio, A. Bottino, G. Capannelli, and P. Piaggio, J. Membr. Sci. **210**, 315 (2002).

[22] M. P. Silva, C. M. Costa, V. Sencadas, A. J. Paleo, and S. Lanceros-Mendez, J. Polym. Res. **18**, 1451 (2011).
[23] P. Martins, C. M. Costa, and S. Lanceros-Mendez, Appl. Phys. A **103**, 233 (2011).
[24] I. S. Elashmawi, E. M. Abdelrazek, H. M. Ragab, and N. A. Hakeem, Physica B **405**, 94 (2010).
[25] V. S. Yadav, D. K. Sahu, S. Y. Singh, M. Kumar, and D. C. Dhubkarya, AIP. Conf. Proc. **1285**, 267 (2010).
[26] C. W. Tang, B. Li, L. Sun, B. Lively, and W. H. Zhong, Eur. Polym. J. **48**, 1062 (2012).
[27] T. Kimura, S. Kawamoto, I. Yamada, M. Azuma, M. Takano, and Y. Tokura, Phys. Rev. B **67**, 180401 (2003).
[28] M. A. Zurbuchen, T. Wu, S. Saha, J. Mitchell, and S. K. Streiffer, Appl. Phys. Lett. **87**, 232908 (2005).
[29] V. Kochervinskii, I. Malyshkina, N. Gavrilova, S. Sulyanov, and N. Bessonova, J. Non-Cryst. Solids **353**, 4443 (2007).
[30] C. V. Chanmal and J. P. Jog, Express Polymer Letters **2**, 294 (2008).
[31] H. Rekik, Z. Ghallabi, I. Royaud, M. Arous, G. Seytre, G. Boiteux, and A. Kallel, Composites:Part B **45**, 1199 (2013).
[32] W. Zhou, Y. Zuo, and W. Ren, Composites:Part A **43**, 658 (2012).
[33] A. Hassen, T. Hanafy, S. E. Sayed, and A. Himanshu, J. Appl. Phys. **110**, 114119 (2011).
[34] G. E. Pike, Phys. Rev. B **6**, 1572 (1972).